

## Capacitive tunnels in single-walled carbon nanotube networks on flexible substrate

M. Z. Iqbal, M. W. Iqbal, Jonghwa Eom, Muneer Ahmad, and Núria Ferrer-Anglada

Citation: *J. Appl. Phys.* **111**, 063712 (2012); doi: 10.1063/1.3695992

View online: <http://dx.doi.org/10.1063/1.3695992>

View Table of Contents: <http://jap.aip.org/resource/1/JAPIAU/v111/i6>

Published by the [American Institute of Physics](#).

---

### Related Articles

Nanoparticle formation in a cavitation bubble after pulsed laser ablation in liquid studied with high time resolution small angle x-ray scattering

*Appl. Phys. Lett.* **101**, 103104 (2012)

Metal nanoantenna plasmon resonance lineshape modification by semiconductor surface native oxide

*J. Appl. Phys.* **112**, 044315 (2012)

Nanostructured thin manganite films in megagauss magnetic field

*Appl. Phys. Lett.* **101**, 092407 (2012)

Magnetic and dielectric properties of sol-gel derived nanoparticles of double perovskite Y<sub>2</sub>NiMnO<sub>6</sub>

*J. Appl. Phys.* **112**, 044311 (2012)

Universal mechanism for ion-induced nanostructure formation on III-V compound semiconductor surfaces

*Appl. Phys. Lett.* **101**, 082101 (2012)

---

### Additional information on J. Appl. Phys.

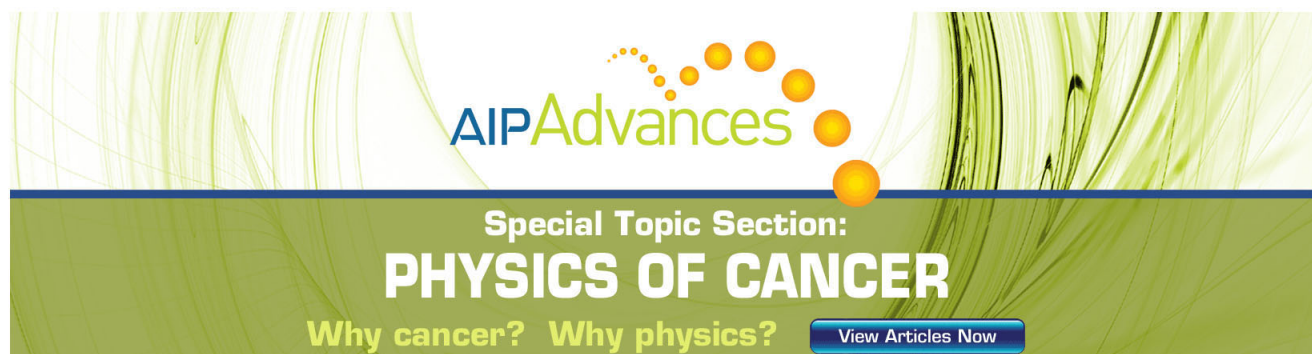
Journal Homepage: <http://jap.aip.org/>

Journal Information: [http://jap.aip.org/about/about\\_the\\_journal](http://jap.aip.org/about/about_the_journal)

Top downloads: [http://jap.aip.org/features/most\\_downloaded](http://jap.aip.org/features/most_downloaded)

Information for Authors: <http://jap.aip.org/authors>

## ADVERTISEMENT

The advertisement features a green background with abstract, flowing lines. At the top, the 'AIP Advances' logo is displayed, with 'AIP' in blue and 'Advances' in green, accompanied by a series of orange dots. Below the logo, the text 'Special Topic Section: PHYSICS OF CANCER' is written in white, with 'PHYSICS OF CANCER' in a larger, bold font. At the bottom, the phrase 'Why cancer? Why physics?' is written in yellow, and a blue button with the text 'View Articles Now' is located on the right side.

**AIP Advances**

Special Topic Section:  
**PHYSICS OF CANCER**

Why cancer? Why physics? [View Articles Now](#)

# Capacitive tunnels in single-walled carbon nanotube networks on flexible substrate

M. Z. Iqbal,<sup>1</sup> M. W. Iqbal,<sup>1</sup> Jonghwa Eom,<sup>1,a)</sup> Muneer Ahmad,<sup>2</sup> and Núria Ferrer-Anglada<sup>3,b)</sup>

<sup>1</sup>*Department of Physics and Graphene Research Institute, Sejong University, Seoul 143-747, South Korea*

<sup>2</sup>*Faculty of Nanotech. and Adv. Mater. Engineering and Graphene Research Institute, Sejong University, Seoul 143-747, South Korea*

<sup>3</sup>*Applied Physics Department, Universitat Politècnica de Catalunya (UPC), Campus Nord B4, J. Girona 3-5, Barcelona 08034, Spain*

(Received 5 September 2011; accepted 22 February 2012; published online 22 March 2012)

We report the analysis of single-walled carbon nanotube networks, which are expected to be suitable as miniaturized flexible radio frequency RC filters and also have important implications for high frequency devices. The surface morphology obtained by atomic force microscopy shows that most of the growth on polypropylene carbonate substrate is homogeneous. The large value of peak intensity ratio of G and D band in Raman spectra indicates the high purity network. Nyquist plots of carbon nanotube networks on a flexible substrate are close to real circles, indicating that the material is conducting, and suggest a simple equivalent circuit having a resistor in parallel with a capacitor. The Bode plots give the dependence of real and imaginary impedances on frequency. While at high frequency, the impedance decreases, due to generation of capacitance between a single-walled carbon nanotube; at low frequency, it shows the normal behavior, having constant value. The tunnels among different carbon nanotubes are capable of storing electric charge. The accumulative capacitances of tunnels for three varied concentrations are calculated by electrochemical impedance spectroscopy simulations to fit the observed Nyquist plots. © 2012 American Institute of Physics. [<http://dx.doi.org/10.1063/1.3695992>]

## I. INTRODUCTION

Thin films made from a single-walled carbon nanotube (SWCNT) network have significant interest in flexible plastic electronics and have become an important research area into the applications of the many electronic devices, which range from metallic to semiconducting carbon nanotubes (CNTs).<sup>1–3</sup> However, the electronic and electrical properties of a collimated CNT are unclear, particularly in the high-frequency regions. Some of these applications are on a single nanotube, some on a bundle of CNTs, and others are based on a composite, whereby CNTs are used to reinforce a desired property of the host material for a specific application.<sup>4–7</sup>

The ac-electrochemical impedance spectroscopy (ac-EIS) has been extensively used to probe mass and charge transport in electrochemical devices, such as chemical sensors,<sup>8</sup> batteries,<sup>9</sup> and fuel cells.<sup>10</sup> The advantages of ac-EIS analysis over the dc analysis include detail characterization of the local electrical behavior of materials. Generally, ac-EIS measurement techniques employing commercially available frequency response analyzers may not be applicable directly to probe kinetic processes occurring in the materials under a driving force. A single impedance spectrum commonly referred to as a “Nyquist plot” or a “Cole-Cole plot” consists of a set of impedance data collected in a wide range of frequency. Due to such a frequency sweep, it is hardly possible to construct the real time Nyquist plots, which are often required for kinetic studies.<sup>11</sup> However, it has been demonstrated<sup>12</sup> that

the construction of Nyquist plots are possible by using one or two data acquisition systems by applying a digitally created arbitrary waveform with various frequency components to the sample, followed by the Fourier transformation of the measured waveform. Incorporating such systems, investigation on the transport kinetics of charge carriers in local areas in a device is, in principle, technically possible at present.

This paper reports the construction of a band-stop filter using a carbon nanotube film due to the existence of capacitive tunnels in network. A SWCNT network grown on plastic substrate shows capacitive behavior under a high alternating current (ac) frequency and is capable of storing an electrical charge.<sup>13,14</sup> In addition, the characteristic of the carbon nanotube film RF filter was simulated with a filter of conventional resistor and capacitor. In the simulated filter, a capacitor and a resistor are in parallel. The magnitude of the parallel resistor critically affected the performance of the capacitor. These SWCNT network films are useful for flexible networks in different fields, including sensors, electrodes, and filters.

## II. EXPERIMENTAL

The conductive network of SWCNT was prepared on the substrate of polypropylene carbonate (PC). The SWCNTs were dissolved in 1% solution of aqueous sodium dodecyl sulfate (SDS), and then the suspension was sonicated for 1 h at 40 W using a probe sonicator. The centrifugal process was done at 14000 rpm for 20 min. The suspension was then vigorously sprayed on the PC substrate, which was heated at 105 °C. The heating of the substrate is done to prevent the agglomeration of SWCNTs networks. After several layers of

<sup>a)</sup>Electronic mail: eom@sejong.ac.kr.

<sup>b)</sup>Electronic mail: nuria@fa.upc.edu.

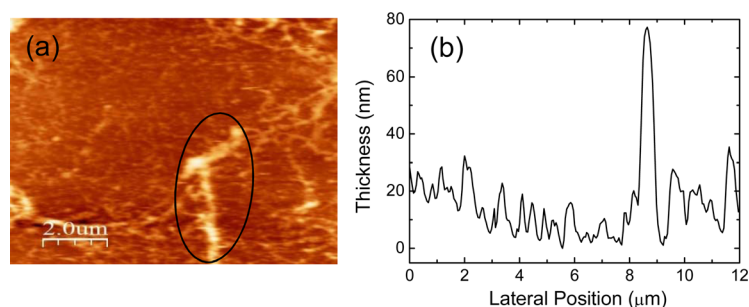


FIG. 1. (a) Topography image of a SWCNT thin film network of which area  $8 \times 8 \text{ m}^2$  for sample S2. (b) The thickness profile taken by drawing the line in the middle of the image.

nanotubes were sprayed onto the PC, the substrate was submerged and shaken in distilled water in order to remove SDS. As a result, a conductive layer is deposited on the PC substrate.<sup>15</sup> Three samples with different densities labeled as S1, S2, and S3 were made for different characterizations. Impedance measurements were performed to determine the functional characteristics of the SWCNT network using an Agilent 4249 A precision impedance analyzer in the range 40 Hz to 110 MHz. The two-probe method was used because SWCNT thin films exhibit high impedance and the contact resistance should be several orders of magnitude lower. Raman spectra were taken using the RENISHAW spectrometer having 633-nm laser wavelength under ambient conditions. Surface morphology is recorded by using the atomic force microscope (NanoFocus Inc.). I-V characteristics' measurements were carried out by four-probe method at room temperature.

### III. RESULTS AND DISCUSSION

#### A. Surface morphology and Raman analysis

The surface morphology is studied by atomic force microscopy (AFM) to verify the dispersion of SWCNTs on PC substrate. As observed from the topography image in Fig. 1(a) for sample S2, the cluster network is distributed on a large area of the PC substrate with mostly uniform thickness. The bright part on the topography image highlighted by the black circle shows a number of clusters agglomerated on that part of the surface.

A thickness profile (Fig. 1(b)) drawn in the middle of the image shows the uniform growth of CNTs on most parts of the grown film, except at the area marked by the black circle. The AFM studies were performed on all the three samples. We observed a similar profile, but the density of clusters is different for each of the three samples in the order  $S1 < S2 < S3$ . The RMS roughness and average thickness for sample S2 are around 12 nm and 35 nm, respectively. Figure 2 shows the Raman spectra for all the three samples, S1, S2, and S3, prepared on flexible PC substrate. The most characteristic features in Raman spectra of SWCNTs were reported by Reich *et al.*<sup>16</sup> While the peak at the high energy range of  $1550 \sim 1650 \text{ cm}^{-1}$  belongs to the tangential G mode, a peak between  $1200$  and  $1400 \text{ cm}^{-1}$  is related to the inter-band with defect-induced vibration (D-mode). As observed in Fig. 2, the appearance of a resonant Raman mode located at  $1726 \text{ cm}^{-1}$  is related to the vibrations of linear carbon chains due to the merging of SWCNTs. This mode is termed as the coalescence-inducing mode (CIM),

because it initiates the coalescence process during thermal treatment of the film.<sup>17</sup>

#### B. Room temperature impedance analysis

To analyze the electronic characteristics in the CNT network, the impedance measurements were employed on rectangular shape samples with length and width 1.5 and 0.5 cm, respectively, at room temperature. The charge carrier transport through this kind of network is thought to be limited not by the conductivity along the nanotubes themselves, but by the large inter-tube resistance associated with barriers to charge propagation that arises at the tube-tube junctions. The highest reported conductivity of a nanotube film reported to date is  $1600 \text{ S/cm}$ ,<sup>18</sup> about three orders of magnitude lower than that of a single nanotube. However, the conductivity is enough for a range of applications. As expected for a network with significant randomness, the impedance is concentration-, frequency-, and density-dependent, but the dependence on density of SWCNTs is distinctively different from that observed for the two other parameters. The two-dimensional Bode plots for the real component ( $Z'$ ) and the imaginary part ( $Z''$ ) are shown in Figs. 3(a) and 3(b), respectively. As observed from Fig. 3(a) at low frequencies, the impedance increases as the density of SWCNT network decreases. The impedance remains constant up to a certain frequency and then starts to decrease at a constant rate. The cut-off frequency in Bode plots is related to the mean distance of the gaps in random nanotube networks.<sup>19</sup> Since the gaps between CNTs act as a parallel plate capacitor, the capacitance contributes to the decrease of impedance at higher frequency. The merging of CNTs during the heat treatment leads to non-conductive isolation,

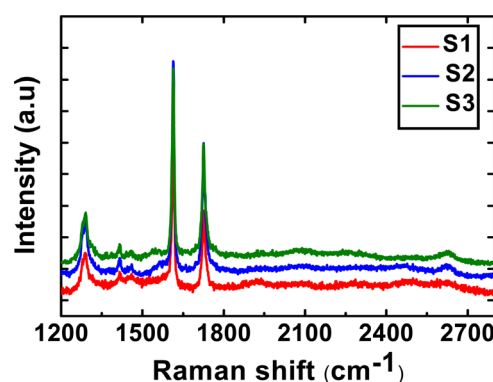


FIG. 2. Raman spectra of SWCNT thin film networks on PC substrate for samples S1, S2, and S3 with different densities.

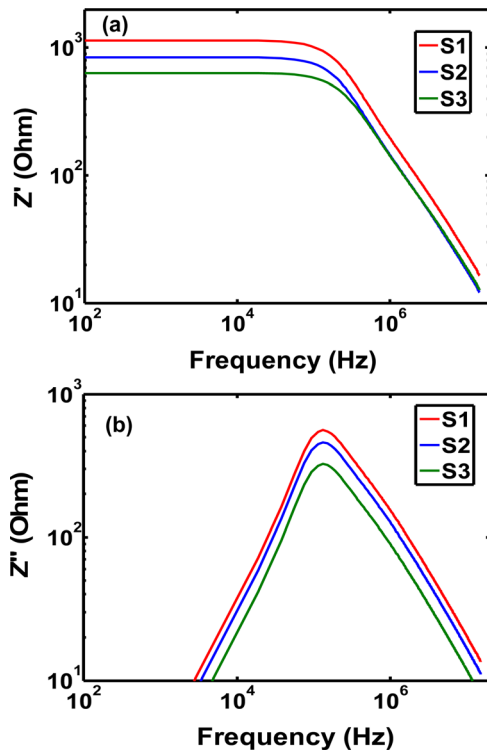


FIG. 3. Bode plots showing the real (a) and imaginary (b) parts of impedance as a function of frequency for SWCNT thin film networks with different density of samples S1, S2, and S3.

providing a medium for capacitance. In addition, some residue of SDS remains in the CNT network to act as a dielectric medium. In the Bode plot, the imaginary component ( $Z''$ ) increases from  $10^3$  to  $10^5$  Hz, and both real and imaginary parts of impedance remarkably decrease as the frequency increases to  $10^7$  Hz.

As can be seen in Fig. 4(a), the complex impedance variation with frequency follows an approximately real circle resembling Debye relaxation peak.<sup>20</sup> At low densities, these conducting networks contain some highly resistive nanotubes, while at higher density, pathways are formed among metallic nanotubes. This can be described<sup>21</sup> with a model that includes both semiconducting and metallic pathways. These ideas have been elaborated by other groups.<sup>22,23</sup> All of these models are based on the inherent randomness and driven charge transport across arbitrary barriers. The SWCNT networks can serve as semiconducting channels when the density is close to the percolation threshold, and they serve also as a metallic interconnect or as a conducting sheet for high network densities. These results can be simulated by a simple equivalent circuit composed of parallel combination of a resistor and a capacitor [inset in Fig. 4(a)]. The contribution of resistance and capacitance is calculated by using electrochemical impedance spectroscopy simulations (EIS), as shown in Figs. 4(b)–4(d), respectively. While the simulated resistances ( $R$ ) are obtained as 550, 418, and 338  $\Omega$  for three samples S1, S2, and S3, the accumulation capacitances are calculated as  $1.89 \times 10^{-9}$ ,  $5.16 \times 10^{-9}$ , and

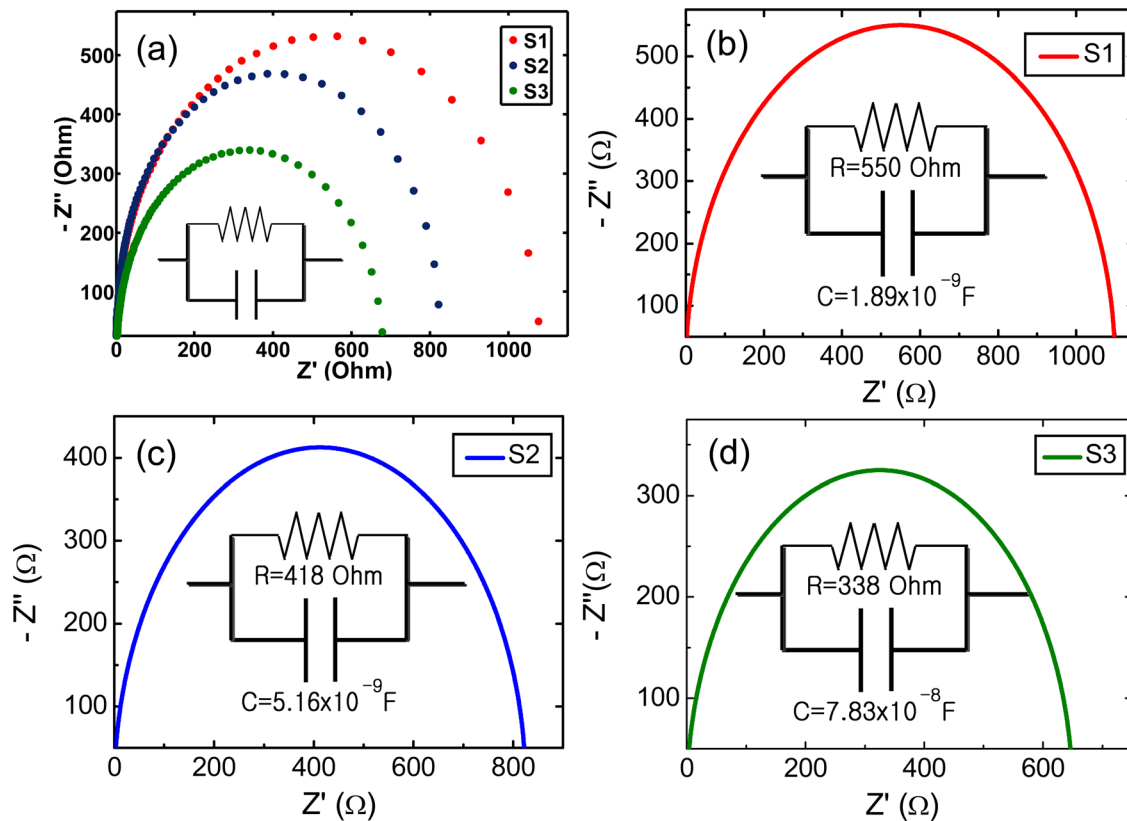


FIG. 4. (a) Nyquist plot showing the real part ( $Z'$ ) vs imaginary part ( $-Z''$ ) of impedance of SWCNT thin film networks with different densities of samples S1, S2, and S3. Inset shows a simple equivalent circuit composed of parallel combination of resistor and capacitor. The electrochemical impedance spectroscopy (EIS) simulation plot (b) for sample S1 with resistance  $R = 550 \text{ } \Omega$  and capacitance  $C = 1.89 \times 10^{-9} \text{ F}$ , (c) for sample S2 with resistance  $R = 418 \text{ } \Omega$  and capacitance  $C = 5.16 \times 10^{-9} \text{ F}$ , and (d) for sample S3 with resistance  $R = 338 \text{ } \Omega$  and capacitance  $C = 7.83 \times 10^{-8} \text{ F}$ .



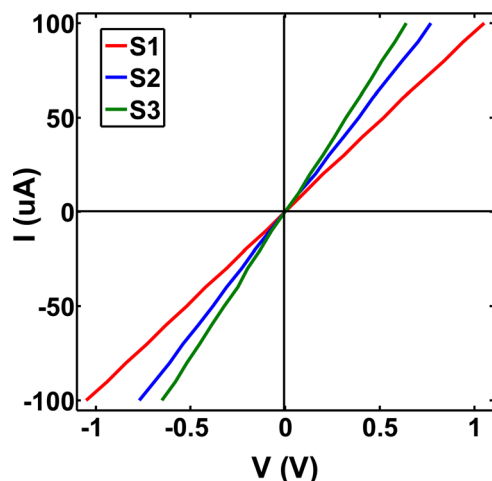


FIG. 5. I-V characteristics of samples S1, S2, and S3 with different densities at room temperature.

$7.83 \times 10^{-8}$  F, respectively. The results presented above indicate that band-stop RC flexible filters can be assembled successfully from a carbon nanotube film grown on a flexible substrate. The range of the cut-off frequency can be tuned by varying the density of SWCNTs networks.

### C. I-V characteristics

As observed from Fig. 5, the I-V plots show Ohmic behavior for all the three samples, S1, S2, and S3. But, for a less dense network, the graph shows slightly resistive nature due to a less percolative SWCNT network, as shown in Fig. 5 for sample S1. The samples with highly dense SWCNT networks show the features, like a more conductive character, as shown in Fig. 5 for samples S2 and S3. For a highly dense network of SWCNTs, the number of tunneling barriers are small and the number of electrical paths with lower resistance rapidly increases. The accumulated number of tunneling barriers does not represent the total number of physical barriers existing in the sample between the electrodes. Some of the barriers are short-circuited due to percolation of SWCNTs and bundles of SWCNTs in some regions.<sup>24</sup>

## IV. CONCLUSIONS

Single-walled carbon nanotube films with different densities were grown on the PC flexible substrate. AFM analysis shows the large area growth of SWCNTs with uniform thickness on most parts of the substrate. The high value of the G/D peak ratio in the Raman spectra confirms the purity of the grown films. The sharp decrease in impedance obtained by the Bode plots is associated with the mean distance of the gaps in CNT networks. At high frequencies, these gaps behave like parallel plate capacitors and cause a decrease in impedance. While the real component of impedance ( $Z'$ ) shows a constant behavior in the frequency range from  $10^2$  to  $10^5$  Hz, the imaginary component of impedance ( $Z''$ ) increases in the frequency range from  $10^3$  to  $10^5$  Hz. Each

component of impedance decreases rapidly as the frequency range of  $10^5$  to  $10^7$  Hz, showing ideal dielectric characteristics. The Nyquist diagram suggests a simple equivalent circuit composed of a parallel combination of a resistor and a capacitor. The simulated values for these RC circuits fit well with experimental data. The films should be a plausible candidate for a flexible band-stop filter. These results offer a new idea for the applications of CNTs to flexible electronic devices.

## ACKNOWLEDGMENTS

This work is supported by Converging Research Center Program through the Ministry of Education, Science and Technology (2011K000620). This work is also supported by Basic Science Research Program (2009-0072022), Mid-career Researcher Program (2010-0010861) and Priority Research Centers Program (2010-0020207) through the National Research Foundation of Korea (NRF) funded by the Ministry of Education, Science and Technology.

- <sup>1</sup>D. Sun, M. Y. Timmermans, Y. Tian, A. G. Nasibulin, E. I. Kauppinen, S. Kishimoto, T. Mizutani, and Y. Ohno, *Nature Nanotechnol.* **6**, 156 (2011).
- <sup>2</sup>N. A. Prokudina, E. R. Shishchenko, O.-S. Joo, K.-H. Hyung, and S.-H. Han, *Carbon* **43**, 1815 (2005).
- <sup>3</sup>J.-H. Shin, D. W. Shin, S. P. Patole, J. H. Lee, S. M. Park, and J. B. Yoo, *J. Phys. D: Appl. Phys.* **42**, 045305 (2009).
- <sup>4</sup>K. P. Ryan, M. Cadek, V. Nicolosi, D. Blond, M. Ruether, G. Armstrong, H. Swan, A. Fonseca, J. B. Nagy, W. Maser, W. Blau, and J. Coleman, *Compos. Sci. Technol.* **67**, 1640 (2007).
- <sup>5</sup>A. A. Sanchez, E. Bermejo, M. Chicharro, A. Zapardiel, G. Luque, N. Ferreyra, and G. A. Rivas, *Anal. Chim. Acta* **577**, 183 (2006).
- <sup>6</sup>H. Huang, W. K. Zhang, X. P. Gan, C. Wang, and L. Zhang, *Mater. Lett.* **61**, 296 (2007).
- <sup>7</sup>V. Gupta and N. Miura, *J. Power Sources* **157**, 616 (2006).
- <sup>8</sup>Y. Li, and S. M. Chen, *Int. J. Electrochem. Sci.* **7**, 2175 (2012).
- <sup>9</sup>E. Karden, S. Buller, and R. W. De Doncker, *Electrochim. Acta* **47**, 2347 (2002).
- <sup>10</sup>J. M. Hawkins, *16th International Telecommunications Energy Conference*, 1994. INTELEC 94, Vancouver, BC, Canada, 30 October–3 November 1994, p. 263.
- <sup>11</sup>A. Searle and L. Kirkup, *Physiol. Meas.* **20**, 103 (1999).
- <sup>12</sup>G. S. Popkurov and R. N. Schindler, *Rev. Sci. Instrum.* **63**, 5366 (1992).
- <sup>13</sup>A. S. Kotosonov, D. V. Shilo, and A. P. Moravskii, *Phys. Solid State* **44**, 666 (2002).
- <sup>14</sup>P. C. Watts, W. K. Hsu, D. P. Randall, V. Kotzeva, and G. Z. Chen, *Chem. Mater.* **14**, 4505 (2002).
- <sup>15</sup>E. Artukovic, M. Kaempgen, D. S. Hecht, S. Roth, and G. Gruner, *Nano Lett.* **5**, 757 (2005).
- <sup>16</sup>S. Reich, C. Thomsen, and J. Maultzsch, *Carbon Nanotubes: Basic Concepts and Physical Properties* (Wiley-VCH, Berlin, 2004), p. 135.
- <sup>17</sup>M. Endo, Y. A. Kim, T. Hayashi, H. Muramatsu, M. Terrones, R. Saito, F. Villalpando-Paez, S. G. Chou, and M. S. Dresselhaus, *Small* **2**, 1031 (2006).
- <sup>18</sup>G. Gruner, *Mater. Res. Soc. Symp. Proc.* **905**, 0905-DD06-05 (2005).
- <sup>19</sup>N. Ferrer-Anglada, J. Perez-Puigdemont, and S. Roth, *Phys. Status Solidi B* **245**, 2276 (2008).
- <sup>20</sup>M. Fukuhara, M. Seto, and A. Inoue, *Appl. Phys. Lett.* **96**, 043103 (2010).
- <sup>21</sup>L. Hu, D. S. Hecht, and G. Gruner, *Nano Lett.* **4**, 2513 (2004).
- <sup>22</sup>J. Vavro, J. M. Kikkawa, and J. E. Fischer, *Phys. Rev. B* **71**, 155410 (2005).
- <sup>23</sup>E. Bakyarova, M. E. Itkis, N. Cabrera, B. Zhao, A. Yu, J. Gao, and R. C. Haddon, *J. Am. Chem. Soc.* **127**, 5990 (2005).
- <sup>24</sup>B. Vigolo, C. Coulon, M. Maugey, C. Zakri, and P. Poulin, *Science* **309**, 920 (2005).